Anharmonic effective pair potentials in $CaTiO_3$, $SrTiO_3$ and $CaGeO_3$ perovskite

Akira Yoshiasa,[a*] Kenji Nakajima,[a] Kei-ichiro Murai[a] and Maki Okube[a]

[a]*Department of Earth and Space Science, Graduate School of Science, Osaka University, Osaka 560-0043, Japan*
Email:yoshiasa@ess.sci.osaka-u.ac.jp

The temperature dependence of EXAFS Debye-Waller factors in $CaTiO_3$, $SrTiO_3$ and $CaGeO_3$ perovskite was investigated with the cumulant expansion method. The $CaGeO_3$ perovskite as an analogue of the Earth's lower-mantle mineral was synthesized in a cubic anvil type apparatus under 10 GPa 1250 K. The Ca, Ti and Ge K-edge EXAFS spectra were measured in transmission mode at temperature up to 1100 K. The effective pair potentials, $V(u)= \alpha u^2/2+ \beta u^3/3!$, were evaluated and the Grüneisen parameter were calculated. The potential coefficients α and β for Ti-O bond in $CaTiO_3$ are 6.9 eVÅ^{-2} and -38 eVÅ^{-3}, respectively. Those for Ge-O bond in $CaGeO_3$ are 9.8 eVÅ^{-2} and -36 eVÅ^{-3}, respectively.

KEYWORDS: EXAFS Debye-Waller factor, anharmonic effective pair potential, perovskite, metastable $CaGeO_3$, $SrTiO_3$

1. Introduction

High-pressure modification of silicate minerals such as perovskite type $Mg_{1-x}Fe_xSiO_3$ and $CaSiO_3$ could be the dominant phases in the Earth's lower mantle, so detailed knowledge of their structures and thermal properties is of great importance for understanding the state of the deep mantle. Also, metagermanates are useful as structural analogs of silicate minerals at high pressures because high pressure perovskite type phases exist at lower pressures.

The ideal perovskite type structure is cubic symmetry such as $SrTiO_3$. Many perovskite type compounds (including the mineral perovskite, $CaTiO_3$, itself) have distorted variants with lower symmetry. $MgSiO_3$ perovskite is orthorhombic (Spacegroup Pbnm) and isotypic with $CaTiO_3$ and $CaGeO_3$ perovskite. The structures are distorted through the tilting and distortion of polyhedra.

At ambient pressure, metastable high pressure $MgSiO_3$ and $CaGeO_3$ perovskite type phases back-transform to stable polymorphs with heating. The transient amorphous phase appears during back-transformation, before recrystallization of stable phase occurs at higher temperatures. The metastable $CaGeO_3$ perovskite undergoes a phase transformation to an amorphous phase at 930 K. Andrault et al. (1996) found that in the CaGeO3 perovskite the apparent Ge-O bond distance determined by the EXAFS analysis using a harmonic model decreases with increasing temperature. They pointed out that the anomalous behavior of local Ge-O bond distance is characteristic of the increase of Ge-O bond anharmonicity in octahedron with increasing temperature. On the other hand, Sicron et al. (1994) measured the temperature dependence of the local structure of perovskite type $PbTiO_3$ ferroelectrics using the EXAFS method. They reported that no significant anharmonicity in thermal vibration for Ti-O bonds was revealed in their parameter fitting.

In this study, we have succeeded in the precise local structure analysis around Ca, Ti and Ge in $CaTiO_3$, $SrTiO_3$ and $CaGeO_3$ perovskite type compounds. The analysis of temperature-dependent EXAFS Debye-Waller factor allows us to evaluate the anharmonicity of effective pair potentials and the interatomic force constants for neighboring atoms (Yoshiasa et al., 1998 and Yoshiasa & Maeda, 1999). In order to study if the anharmonic thermal vibration in metastable structure is prominent, we have determined the temperature variation of the local structural parameters in stable and metastable perovskite at temperature up to 1100 K.

2. Experimental and analysis

The $CaGeO_3$ perovskite was synthesized in a cubic anvil type apparatus under 10 GPa 1250 K. The crystals of $CaTiO_3$, $SrTiO_3$ and $CaGeO_3$ perovskite were identified by X-ray diffraction. The appropriate amount of fine powder sample and boron nitride powder was mixed and pressed into pellets of <0.2 mm in thickness and 10.0 mm in diameter. All samples had edge-jumps with 0.7 ($\Delta \mu d$), where μ is the linear absorption coefficient and d is the thickness. The measurements of Ca, Ti and Ge K-edge EXAFS spectra were carried out in the transmission mode at beam line BL-7C of the Photon Factory in KEK, Tsukuba (Proposal No. 98G319). All X-ray absorption measurements in the temperature range from 300 to 1100 K were made under a helium atmosphere. The synchrotron radiation was monochromatized by a Si(111) double crystal monochromator. Mirrors are used to eliminate higher harmonics. Details of the measurement and analysis were given in reference (Yoshiasa *et al.*, 1997 and Yoshiasa *et al.*, 1999b).

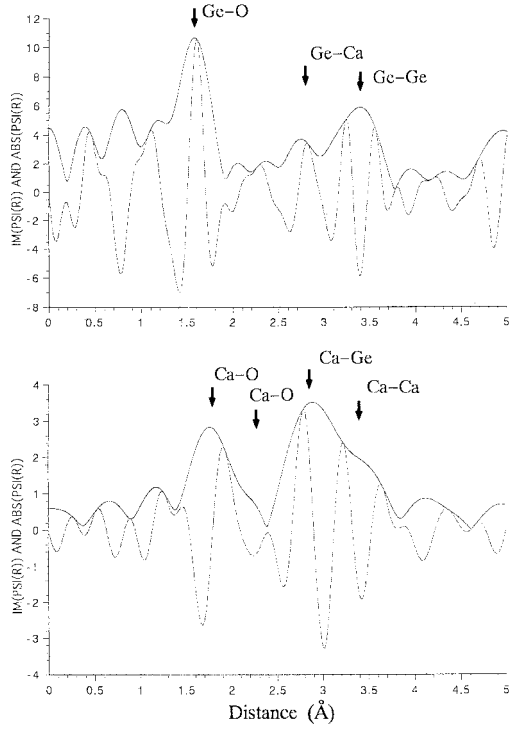

Figure 1. Fourier transforms of the Ge and Ca K-edge EXAFS for $CaGeO_3$ perovskite at 500 K. No phase shift corrections are made.

The EXAFS interference function, $\chi(k)$, was extracted from the measured absorption spectra using the standard procedure (Maeda, 1987). The $\chi(k)$ was normalized using MacMaster coefficients according to the EXAFS workshop report (Lytle et al. 1989). Figure 1 shows examples of Fourier transforms of the Ca and Ge K-edge EXAFS spectra in the ranges of $3.5<k<11.5$ for Ca and of $3.5<k<14.0$ for Ge. In quantitative analyses we carried out the Fourier-filtering technique and a nonlinear least-squares fitting method by comparing the observed $\chi(k)_{exp}$ and calculated $\chi(k)_{calc}$. We used the EXAFS formula in the single scattering theory with the cumulant expansion up to the fourth order term (Ishii, 1992):

$$\chi(k) = \sum_B (N_B / kR^2_{AB}) \left| f_B(k;\pi) \right| \exp(-2R_{AB}/(k/\pi)) \exp(-2\sigma 2k^2 + (2/3)\sigma 4k^4)$$
$$\times \sin(2kR_{AB} - (2k/R_{AB})(1 + 2R_{AB}/(k/\eta)) \sigma 2 - (4/3)\sigma 3k^3 + \psi_{AB}(k)) \quad \ldots(1)$$

where N_B is the coordination number of scattering atoms B at distance R_{AB} from the absorbing atom A, $|f_B(k; \pi)|$ the backscattering amplitude of photoelectrons and $\psi_{AB}(k)$ the phase shift function. Values of the function $|f_B(k; \pi)|$ and $\psi_{AB}(k)$ were calculated using the FEFF3 program (Rehr et al. 1991). σ n denotes the nth cumulant. The mean free path λ of the photoelectron is assumed to depend on the wave number, $\lambda(k)=k/\eta$, where η is a constant.

Single-shell fitting was carried out for each nearest-neighbor distance, where the number of neighboring atoms was fixed at the crystallographic value as N_B=6 for the Ti-O and Ge-O distances, N_B=8 for the Ca-O distances and N_B=6 for the Ti-Ti and Ge-Ge distances. We assumed that η and ΔE_0 have negligible temperature dependence. Here ΔE_0 is the difference between the theoretical and experimental threshold energies. The values of η and ΔE_0 are determined so as to give the best fit to the spectrum at the lowest temperatures. Because the fourth-order term was negligible, the refinement was performed to the structure parameters R_{AB}, $\sigma 2$ and $\sigma 3$ in each shell by use of the fixed η and ΔE_0 values. The reliability of fit parameters,

$$R = \sum_S \left| k_s^3 \chi(k_s)_{exp} - k_s^3 \chi(k_s)_{calc} \right| / \left| k_s^3 \chi(k_s)_{exp} \right|,$$

between the experimental and calculated EXAFS functions was less than 0.081. The quality of fit between $k^3\chi_{exp}$ and $k^3\chi_{calc}$ is shown in Fig 2.

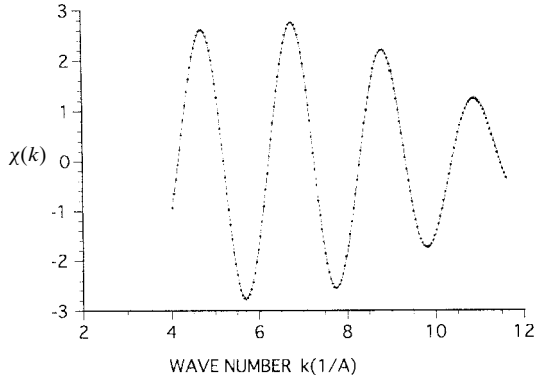

Figure 2. Fourier-filtered EXAFS spectra (dotted curve) and least-squares fit (solid curve) for first-nearest Ti-O distance in $CaTiO_3$ at 600 K.

3. Results and Discussion

3.1 Temperature dependence of the Ti-O and Ge-O distance.

Figure 3 shows the temperature dependence of the Ti-O and Ge-O bond distances in $CaTiO_3$, $SrTiO_3$ and $CaGeO_3$ perovskite. The Ti and Ge atoms in $CaTiO_3$ and $CaGeO_3$ have three kinds of first nearest-neighbor distances which are crystallographically nonequivalent with each other. The difference in distance among these nonequivalent bonds is within 0.009 Å. Obtained local bond distances of 1.960(4) Å for Ti-O bonds and 1.894(1) Å for Ge-O bonds agreed closely with those by single crystal X-ray structure analysis (Sasaki et al. 1987 and Sasaki et al. 1983). Six Ti-O distances in $SrTiO_3$ (1.952(2) Å) are crystallographically equivalent with each other.

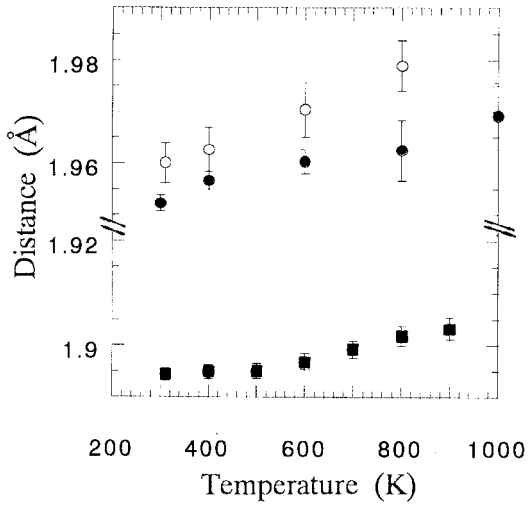

Figure 3. Temperature dependence of the Ti-O bond in $CaTiO_3$ (°), Ti-O bond in $SrTiO_3$ (•) and Ge-O bonds in $CaGeO_3$ (▪).

The harmonic approximation ignores anharmonic contributions and requires a cumulant up to only second order term. As can be seen from the equation (1), the third order term correlates largely with the distance and phase-shift function. For an anharmonic compound, the obtained distance with a harmonic model shifts apparently to a shorter distance due to the neglect of the third-order term (Yoshiasa et al. 1990). The apparent local Ge-O bond distance with a harmonic model (Andrault et al. 1996), therefore, decreased with increasing temperature.

Table I. Potential parameters and Grüneisen parameters γ_G for the Ti-O and Ge-O bonds in $CaTiO_3$, $SrTiO_3$ and $CaGeO_3$ perovskite.

	$CaTiO_3$	$SrTiO_3$	$CaGeO_3$
R_0 (Å)	1.95	1.95	1.89
α (eV/Å^2)	6.9(1)	7.1(1)	9.8(1)
β (eV/Å^2)	-38(2)	-27(2)	-36(2)
γ_G	1.8	1.3	1.2

3.2 Anharmonic effective pair potentials and Grüneisen parameters for Ti-O and Ge-O bonds in octahedra

Figure 4 shows the temperature dependence of $\sigma 2$ and $\sigma 3$ for Ti-O and Ge-O bonds in $CaTiO_3$, $SrTiO_3$ and $CaGeO_3$ perovskite. The Debye-Waller type factor $\sigma 2$ includes the effects of static and dynamic disorders. The static disorder is the configuration disorder, while the dynamic disorder arises from the thermal vibration of atoms. The contribution of the thermal vibration, $\sigma_{thermal}$, can be estimated under the assumption of classical statistical dynamics by the temperature dependence of $\sigma 2$ (Yoshiasa et al., 1999a). A steep slope in the figure represents a weak bonding. The gradient for the experimental $\sigma 2$ is equal to k_B/α, if we evaluate the anharmonic effective pair potential $V(u)= \alpha u^2/2+\beta u^3/3!$ from the contribution to the thermal vibration, where k_B is the Boltzmann constant, α and β are the potential coefficients and u is the deviation of the bond distance from the location of the potential minimum. β is calculated from the values of $\sigma 2$ and $\sigma 3$ (Ishii, 1994). Calculated potential parameters are listed in Table I. The potential coefficients α for the Ti-O bonds in $CaTiO_3$ and $SrTiO_3$ are 6.9 and 7.1 eV/Å^2, respectively. The potential coefficient α for the Ge-O bond in $CaGeO_3$ is 9.8 eV/Å^2. The Grüneisen parameters γ_G (Table 1) were calculated from potential parameters α and β (Yoshiasa & Maeda,

1999). The derived values refer to short-range correlation of the atomic motion. The derived Grüneisen parameters have normal values. The value for Ge-O bond is smaller than those for Ti-O bonds.

Figure 5 shows the anharmonic effective pair potentials for Ti-O bond in $CaTiO_3$ and for Ge-O bond in $CaGeO_3$. The effective pair potential for Ti-O bond in stable $CaTiO_3$ is asymmetric and broader than that in metastable $CaGeO_3$. The effective pair potential for Ti-O bonds in $SrTiO_3$ is also asymmetric. It is known that an anharmonic contribution to the EXAFS Debye-Waller factor in many compounds appears pronouncedly when the magnitude of $\sigma 2$ is greater than 0.01 Å^2 (Yoshiasa et al.1997). The magnitude of $\sigma 2$ of Ti-O bonds in perovskites at higher temperature is greater than 0.01 Å^2. It can be pointed out that the Ti-O bonds in $PbTiO_3$ (Sicron et al., 1994) at higher temperature should also be anharmonic because temperature gradient for the experimental $\sigma 2$ for Ti-O bond in $PbTiO_3$ is similar to those in $CaTiO_3$ and $SrTiO_3$. The Si-O bonds in the perovskite type $MgSiO_3$ and $CaSiO_3$ should be anharmonic in the Earth's lower mantle conditions.

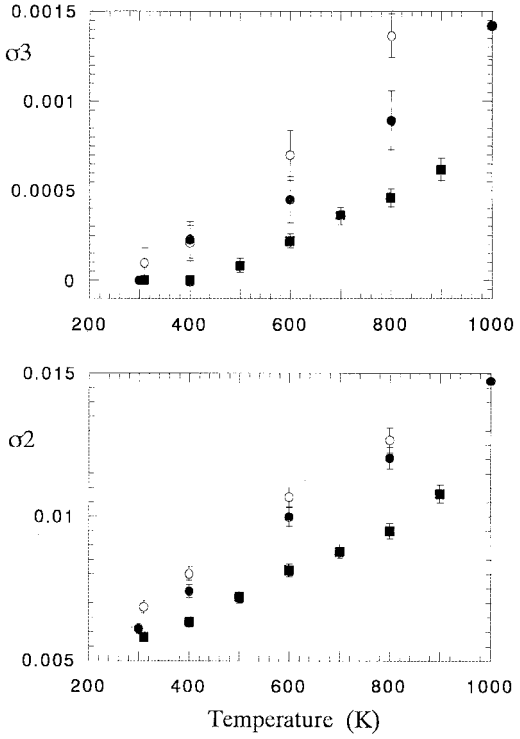

Figure 4. Temperature dependence of $\sigma 2$ and $\sigma 3$ for Ti-O bond in $CaTiO_3$ (°), for Ti-O bonds in $SrTiO_3$ (•) and for Ge-O bond in $CaGeO_3$ (▪).

3.3 EXAFS Debye-Waller factors and potential coefficients for Ca-O, Ti-Ti and Ge-Ge distances

Figure 6 shows the temperature dependence of $\sigma 2$ for the Ca-O distances (2.55(1) and 2.49(1) Å at 500 K in $CaTiO_3$ and $CaGeO_3$, respectively), Ti-Ti distance (3.836(5) Å at 600 K in $CaTiO_3$) and Ge-Ge distance (3.731(3) Å at 600 K in $CaGeO_3$). The potential coefficients α for the Ca-O distances in $CaTiO_3$ and $CaGeO_3$ are 4.3 and 4.9 eV/Å^2, respectively. The potential coefficients α for the Ti-Ti and Ge-Ge distances in $CaTiO_3$ and $CaGeO_3$ are 8.0 and 7.4 eV/Å^2, respectively. It is interesting to show that the gradients of $\sigma 2$ for the Ca-O distances are larger than those for the Ti-Ti and Ge-Ge distances in $CaTiO_3$ and $CaGeO_3$: the potential coefficients for the Ca-O distances are significantly smaller than those for the longer Ti-Ti or Ge-Ge distances though the potential coefficient decreases usually as a result of the larger bond distance. The Ca-O bonds in perovskite type compounds have relatively larger mean square amplitudes of vibration than those for Ti-Ti or Ge-Ge distances as judged by each value of potential coefficients.

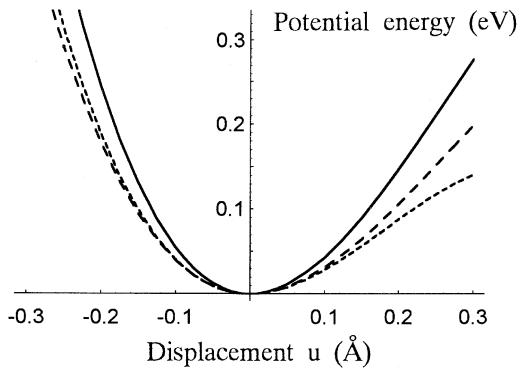

Figure 5. Anharmonic effective pair potentials for Ti-O bond in $CaTiO_3$ (dotted line), for Ti-O bond in $SrTiO_3$ (dashed line) and for Ge-O bond in $CaGeO_3$ (straight line).

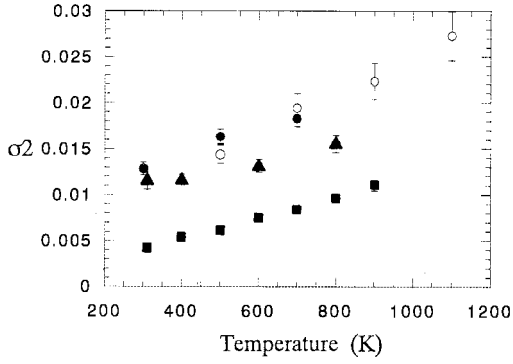

Figure 6. Temperature dependence of $\sigma 2$ for Ca-O distance in $CaTiO_3$ (°), for Ca-O distance in $CaGeO_3$ (•), for Ti-Ti distance in $CaTiO_3$ (▲) and for Ge-Ge distance in $CaGeO_3$ (▪).

References

Andrault, D., Itié J.-P. & Farges, F. (1996) Amer. Mineral. **81** 822-832
Ishii, T. (1992) J. Phys : Condens. Matter **4** 8029-8034
Ishii, T. (1994) Principle of the theory of EXAFS, Shokabo, Tokyo
Lytle, F.W., Sayers, D.E. & Stern, E.A. (1989) Physica **B158** 701-722
Maeda, H. (1987) J. Phys. Soc. Jpn. **56** 2777-2787
Rehr, J.J., Mustre de Leon, J. Zabinski, S.I. & Albers, R.C. (1991) Am. Chem. Soc. **113** 5135-5140
Sasaki, S., Prewitt, C.T. & Liebermann, R.C. (1983) Amer. Mineral. **68** 1189-1198
Sasaki, S., Prewitt, C.T. & Bass, J.D. (1987) Acta Cryst. **C43** 1668-1674
Sicron, N., Ravel, B. Yacoby, Y., Stern, E.A., Dogan, F. & Rehr, J.J. (1994) Phys. Rev. **B50** 13168-13180
Yoshiasa, A., Maeda, H., Ishii, T. & Koto, K. (1990) Solid State Ionics **40/41** 341-344
Yoshiasa, A., Koto, K., Maeda, H. & Ishii, T. (1997) Jpn. J. Appl. Phys. **36** 781-784
Yoshiasa, A., Nagai, T., Murai, K., Yamanaka, T., Kamishima, O. & Shimomura, O. (1998) Jpn. J. Appl. Phys. **37** 728-729
Yoshiasa, A., Nagai, T., Ohtaka, O., Kamishima, O. & Shimomura, O. (1999a) J. Synchrotron Rad. **6** 43-49
Yoshiasa, A., Tamura, T., Kamishima, O., Murai, K., Ogata, K. & Mori, H. (1999b) J. Synchrotron Rad. **6** 1051-1058
Yoshiasa, A. & Maeda, H. (1999) Solid State Ionics **121** 175-182